PHYSICAL REVIEW B VOLUME 21, NUMBER 2 15 JANUARY 1980

Optical response of metals in a number-conserving relaxation-time approximation

P. Garik and N. W. Ashcroft
Laboratory of Atomic and Solid State Physics and Materials Science Center, Cornell University, Ithaca, New York 14853
(Received 2 August 1979)

The electronic transport equations for a periodic solid are presented in a number-conserving relaxation-time approximation. The inclusion of a phenomenological scattering time and the concurrent imposition of the equation of continuity is shown to lead to quantum-mechanical interference between the scattering mechanism and the primary effects of the periodic crystalline field. In model calculations carried out for the simple metals, the consequences of this interference are examined in the context of both optical interband transitions and the damping of the long-wavelength volume plasmons. An interband contribution to the static conductivity is also found as a direct consequence of the conserving approximation. It can be expressed as a relatively simple function of both scattering time and oscillator strengths. Local-field effects are also discussed within the same model.

I. INTRODUCTION

The shape of absorption curves observed in optical and electron-loss spectroscopy on metals is physically related to the available electronic decay channels. In a real crystal such mechanisms are numerous; they include electron-phonon, electron-electron, electron-impurity, and electron-defect scattering, as well as intrinsic interband (IB) transitions. As a result, both the detailed microscopic calculation of absorption curve widths and comparison to experiment are difficult. It is for this reason that a description of the effects of the different mechanisms via a phenomenological scattering or relaxation time τ is attractive. However, the incorporation of a scattering time to describe electronic transport properties in metals must be carried out with some caution. In particular, within the framework of the random-phase approximation (RPA), Ehrenreich and Philipp[1] have introduced the relaxation time in an *ad hoc* fashion in order to account for the shapes of optical absorption curves. Although their formulation leads to good agreement with experimental data, it nevertheless violates number conservation. More recently, Greene *et al.*[2] and Mermin[3] have formulated theories incorporating the relaxation time in the quantum-mechanical Liouville equation in a manner specifically designed to overcome this problem. In particular, Mermin has succeeded in deriving a Lindhard-type dielectric function for the free-electron gas including a phenomenological relaxation time. It is the purpose of this paper to extend Mermin's approach to the case of electrons moving in the periodic potential of a crystal. In doing so, expressions for the dependence of the local field on scattering have also been derived. These allow us to study the effect on optical absorption and energy-loss line shapes due to both scattering and the local field in the simple metals. Finally, we are able to make a comparison between the present number-conserving results and the previous work in which this consideration has been neglected.

We devote Sec. II of this paper to a reexposition and generalization of the number-conserving quantum-mechanical relaxation-time approximation. In Sec. III the number-conserving longitudinal dielectric function is derived for electrons in a periodic crystal potential and undergoing scattering processes. An application of the result to the optical conductivity in simple metals finds good agreement with the previous results of Ashcroft and Sturm (AS).[4] Furthermore, it is found that because of the band broadening resulting from the introduction of a scattering time, there is a contribution to the dc *conductivity* from interband transitions.

In Sec. IV we present a calculation of the contribution of the local field in our relaxation-time approximation. The derivation follows Wiser's collisionless case procedure.[5] Although the contribution of the local field has been shown to be weak in nearly-free-electron-like metals,[5,6] such a calculation is useful in that the dependence of the local field on the relaxation time is clearly displayed, and we are able to make contact with the approximations of others.[7] An analysis of the local field contribution in terms of interband transitions and the resultant effect on line shapes in the simple metals is shown to be straightforward.

Finally, in Sec. V the number-conserving result is applied to a derivation of expressions for the plasmon dispersion and damping in a periodic potential. Recent work by several authors has shown conclusively that interband transitions are the dominant processes in the damping of plasmons in simple metals.[8-12] Nevertheless, other scattering mechanisms do contribute to the full width at half maximum (FWHM) of the energy-loss function. In the number-conserving relaxation-time approxima-

tion the contribution of both collisions and interband transitions is handled consistently. By doing so, we find that the interband and scattering contributions to the FWHM obey an empirical Matthiessen's rule. However, we also find that the damping, i.e., the imaginary part of the plasmon frequency, is *not* simply related to the FWHM but reflects an interplay between interband transitions and band broadening due to electronic scattering. In our model calculations for the simple metals, we find very good agreement between our calculations and experimental results for both the long-wavelength plasma frequency and the FWHM of the energy-loss function.

The formulas developed in Secs. III–V are generally valid for electrons moving in a periodic potential. However, all of the numerical calculations have been carried out for simple metals, i.e., metals well described by a weak pseudopotential, a small core, and a large band gap between the core and conduction electrons. The pseudopotential matrix elements used are either from fitted experimental data or derived from the empty-core potential.[13] Finally, except where otherwise noted, band calculations were carried out using a two-plane wave (2-PW) model and a suitable band effective mass.

II. FORMALISM: THE SINGLE-PARTICLE DENSITY MATRIX

In order to calculate the electronic response properties of our system, we start with the single-particle approximation and assume that the electrons move in a self-consistent (screened) field. Ehrenreich and Cohen[14] have shown that in the absence of collisions, the equation of motion for single-particle density matrix in the presence of a self-consistent field can be obtained from the random-phase approximation of many-body theory.

To describe the system we write the total one-electron Hamiltonian as:

$$\hat{H} = \hat{H}_0 + \hat{H}_1(\vec{r}, \vec{p}, t),$$

where $\hat{H}_0$ describes some unpertrubed system and has associated eigenfunctions $\{|u\rangle\}$ which satisfy:

$$\hat{H}_0|u\rangle = \mathcal{E}_u|u\rangle .$$

The self-consistent perturbation $\hat{H}_1(\vec{r}, \vec{p}, t)$ is taken to be the *screened* external perturbation.

The collisionless single-particle density matrix for the unperturbed system, $\hat{\rho}^{(0)}$, is written

$$\hat{\rho}^{(0)} = \frac{1}{e^{\beta(\hat{H}_0 - \mu_0)} + 1} , \tag{1}$$

where the occupation of a single-particle state is given by

$$\hat{\rho}^{(0)}|u\rangle = f_u|u\rangle = \frac{1}{e^{\beta(\mathcal{E}_u - \mu_0)} + 1}|u\rangle . \tag{2}$$

Here μ_0, the equilibrium chemical potential, is constant throughout the system.

In the presence of an external perturbation *and* any internal interactions as are to be described by collisions, the total single-particle density matrix satisfies the Liouville equation

$$\frac{d\hat{\rho}}{dt} = \frac{1}{i\hbar}[\hat{H}, \hat{\rho}] + \left(\frac{\partial \hat{\rho}}{\partial t}\right)_{\text{coll}} . \tag{3}$$

The difficulty now arises in the selection of an appropriate collision term $(\partial\hat{\rho}/\partial t)_{\text{coll}}$. We proceed to make the standard relaxation-time approximation,[15] i.e., in a time interval dt the probability that any electron in the ensemble will suffer a collision is dt/τ. Now, it is well known that an incautious introduction of such a collision time into either the classical Boltzmann equation or the quantum-mechanical Liouville equation *can* lead to a violation of the equation of continuity, and thence to results which are not number conserving.[16] For the case of otherwise free electrons, Mermin[3] has observed that the difficulty can be traced to the need for a correct description of the particles immediately *after* collisions. Whether we consider jellium or a system with a periodic potential, subsequent to such collisions the single-particle density matrix must represent the fact that the particles are in a state of local equilibrium. This is of course the normal procedure in formulating the semiclassical Boltzmann equation in the relaxation-time approximation. To carry this out for the Liouville equation, we follow Mermin and specify a *local* equilibrium density matrix of the form

$$\hat{\rho}_{\text{loc}} = \frac{1}{e^{\beta(\hat{H} - \mu_0 - \delta\hat{\mu})} + 1} . \tag{4}$$

It is the introduction here of a local chemical potential, $\mu_0 + \delta\hat{\mu}(\vec{r}, t)$, that supplies the additional degree of freedom necessary to achieve number conservation. [We note in passing that $\delta\hat{\mu}(\vec{r}, t)$ is a function of the strength of the scattering as described by τ; however, we suppress explicit representation of this dependence until necessary.]

Essentially we have now reduced the transport to two equations in two unknowns; the Liouville equation of motion and the continuity equation are coupled through the unknown total density matrix $\hat{\rho}$ and the unknown local chemical potential $\delta\hat{\mu}(\vec{r}, t)$ describing the local equilibrium. We now solve this pair of equations.

In the relaxation-time approximation, the equation of motion is

$$\frac{d\hat{\rho}}{dt} = \frac{1}{i\hbar}[\hat{H}, \hat{\rho}] - \frac{1}{\tau}(\hat{\rho} - \hat{\rho}_{\text{loc}}) . \tag{5}$$

At the level of linear-response theory, we use (5) to calculate $\hat{\rho}^{(1)}$, the first-order correction to the unperturbed equilibrium density matrix $\hat{\rho}^{(0)}$. The single-particle unperturbed and interaction Hamiltonians for a particle of charge e are, respectively,

$$\hat{H}_0 = \frac{1}{2m}\left(\vec{p} - \frac{e}{c}\vec{A}_0(\vec{r},t)\right)^2 + e\Phi_0(\vec{r},t) + V(\vec{r}),$$

$$\hat{H}_1 = \frac{e}{2mc}\left[\vec{A}\cdot\left(\vec{p} - \frac{e}{c}\vec{A}_0\right) + \left(\vec{p} - \frac{e}{c}\vec{A}_0\right)\cdot\vec{A}\right] + e\Phi(\vec{r},t). \tag{6}$$

Here $\vec{A}_0(\vec{r},t)$ and $\Phi_0(\vec{r},t)$ are the fields present in the unperturbed system, $V(\vec{r})$ is a general one-body potential energy which may be a crystal potential, and $\vec{A}(\vec{r},t)$ and $\Phi(\vec{r},t)$ are the self-consistent vector and scalar perturbing potentials. As is normal in linear-response theory, terms of order $\vec{A}^2$ have been neglected.

The analysis which now follows is a generalization of Mermin's free-electron procedure. We suppose that $\delta\hat{\mu}(\vec{r},t)$ is first order in the perturbation $\hat{H}_1$. Then to linear order the matrix element of the local equilibrium density matrix is

$$\langle u|\hat{\rho}_{\rm loc}|v\rangle = f_u\delta_{uv} + \left(\frac{f_u - f_v}{\mathcal{E}_u - \mathcal{E}_v}\right)\langle u|\hat{H}_1 - \delta\hat{\mu}(\vec{r},t)|v\rangle + O(\delta\mu^2). \tag{7}$$

From (5) and (6) we find after linearizing that

$$\langle u|\hat{\rho}^{(1)}|v\rangle = \frac{f_u - f_v}{\mathcal{E}_u - \mathcal{E}_v - \hbar(\omega + i/\tau)} \times\left(\langle u|\hat{H}_1|v\rangle - \frac{i\hbar/\tau}{\mathcal{E}_u - \mathcal{E}_v}\langle u|\hat{H}_1 - \delta\hat{\mu}|v\rangle\right). \tag{8}$$

We have expanded here the total density matrix to first order, i.e., $\hat{\rho} = \hat{\rho}^{(0)} + \hat{\rho}^{(1)} + O(\hat{H}_1^2)$.

Recall now that the single-particle current-density operator at a point $\vec{r}$ is $\hat{\vec{j}}(\vec{r},t) = \hat{\vec{j}}^{(0)}(\vec{r}) + \hat{\vec{j}}^{(1)}(\vec{r},t)$, where

$$\hat{\vec{j}}^{(0)}(\vec{r}) = \frac{1}{2m}\left[\vec{p}\,\delta(\vec{r} - \hat{\vec{r}}) + \delta(\vec{r} - \hat{\vec{r}})\vec{p}\right] - \frac{e}{mc}\vec{A}_0(\vec{r},t)\delta(\vec{r} - \hat{\vec{r}})$$

and

$$\hat{\vec{j}}^{(1)}(\vec{r},t) = -\frac{e}{mc}\vec{A}(\vec{r},t)\delta(\vec{r} - \hat{\vec{r}}).$$

Accordingly, to first order the induced current is

$$\delta\hat{\vec{j}}(\vec{r},t) = {\rm Tr}\hat{\rho}^{(1)}\hat{\vec{j}}^{(0)}(\vec{r}) + {\rm Tr}\hat{\rho}^{(0)}\hat{\vec{j}}^{(1)}(\vec{r},t). \tag{9}$$

If we now Fourier transform (9), the longitudinal current is found to satisfy

$$\hat{q}\cdot\delta\vec{j}(\vec{q},\omega) = \frac{-e}{\hbar mc}{\rm Tr}\hat{\rho}^{(0)}\{e^{-i\vec{q}\cdot\vec{r}}[\vec{p}\cdot\vec{A}(\vec{r},\omega) + \vec{A}(\vec{r},\omega)\cdot\vec{p}]\} + \sum_{u,v}\frac{(f_u - f_v)\langle v|e^{-i\vec{q}\cdot\vec{r}}|u\rangle}{\mathcal{E}_u - \mathcal{E}_v - \hbar(\omega + i/\tau)}(\mathcal{E}_u - \mathcal{E}_v)/\hbar \times\left(\langle u|\hat{H}_1|v\rangle - \frac{i\hbar/\tau}{\mathcal{E}_u - \mathcal{E}_v}\langle u|\hat{H}_1 - \delta\hat{\mu}|v\rangle\right). \tag{10}$$

On the other hand, to linear order the induced number density is given by

$$\delta n(\vec{q},\omega) = {\rm Tr}\rho^{(1)}e^{-i\vec{q}\cdot\vec{r}} = \sum_{u,v}\frac{(f_u - f_v)\langle v|e^{-i\vec{q}\cdot\vec{r}}|u\rangle}{\mathcal{E}_u - \mathcal{E}_v - \hbar(\omega + i/\tau)} \times\left(\langle u|\hat{H}_1|v\rangle - \frac{i\hbar/\tau}{\mathcal{E}_u - \mathcal{E}_v}\langle u|\hat{H}_1 - \delta\hat{\mu}|v\rangle\right). \tag{11}$$

Finally, we now impose on $\delta n(\vec{q},\omega)$ and $\delta\vec{j}(\vec{q},\omega)$ the connection required by the equation of continuity:

$$\omega\delta n(\vec{q},\omega) - \vec{q}\cdot\delta\vec{j}(\vec{q},\omega) = 0. \tag{12}$$

After combining (12) with (10) and (11) and Fourier transforming, we arrive at

$$\delta n(\vec{q},\omega) = -\frac{e\tau}{mc}{\rm Tr}\{\rho^{(0)}e^{-i\vec{q}\cdot\vec{r}}[\nabla\cdot\vec{A}(\vec{r},\omega)]\} - \frac{i2e\tau}{\hbar mc}{\rm Tr}[\hat{\rho}^{(0)}\vec{A}(\vec{r},\omega)\cdot(\vec{p} - \hbar\vec{q}/2)] + \sum_{u,v}\frac{f_u - f_v}{\mathcal{E}_u - \mathcal{E}_v}\langle u|\hat{H}_1 - \delta\hat{\mu}|v\rangle\langle v|e^{-i\vec{q}\cdot\vec{r}}|u\rangle. \tag{13}$$

The results which Mermin presented follow from an application of (13) to the free-electron gas for which $|u\rangle$ and $|v\rangle$ are simple plane waves. In the following sections, we consider the consequences of (13) for independent electrons moving in a periodic potential.

III. DIELECTRIC RESPONSE FUNCTION FOR A CRYSTAL

The response theory presented in this section will be restricted to disturbances and responses with wave vector $\vec{q}$ contained within the first Brillouin zone. We will ignore responses of the electron system that represent diffractions by the crystal, i.e., Umklapp processes, of wave vector $\vec{q} + \vec{K}$ for $\vec{K}$, a reciprocal-lattice vector. As has been shown by Ehrenreich,[16] this simplification is equivalent to averaging the fields over many lattice sites *before* evaluating the response functions. We normally refer to this as the macroscopic response of the system. The corrections that result from evaluating the true microscopic response of the

system (i.e., including the higher Fourier components) are dealt with in Sec. IV.

We specialize to a Bravais lattice and write $\hat{H}_0$ as $\hat{H}_0 = p^2/2m + V(\vec{r})$. Here $V(\vec{r})$ is the periodic potential satisfying $V(\vec{r}+\vec{R}) = V(\vec{r})$ for all lattice vectors $\{\vec{R}\}$ of the crystal. Correspondingly, the unperturbed basis set is $\{|u\rangle\} = \{|\vec{k}, l\rangle\}$ with $\vec{k}$ the Bloch wave vector and l the band index. Thus

$$\langle \vec{r}|\vec{k}l\rangle = \frac{1}{\sqrt{\Omega}}\, e^{i\vec{k}\cdot\vec{r}} u_{\vec{k}l}(\vec{r}),$$

where Ω is the crystal volume and $u_{\vec{k}l}(\vec{r})$ is the periodic piece of the Bloch function.

Let us consider the wave-vector and frequency-dependent longitudinal dielectric function appropriate to the linear response of a crystal to, say, the field of a charged particle. If $\Phi(\vec{q}, \omega)$ is the self-consistent potential arising from such a longitudinal disturbance, then by definition we have

$$\vec{q}\cdot\delta\vec{j}(\vec{q},\omega) = \frac{\omega q^2}{4\pi e}[\hat{q}\cdot\vec{\epsilon}(\vec{q},\omega)\cdot\hat{q} - \vec{1}]\Phi(\vec{q},\omega) = \omega\delta n(\vec{q},\omega), \tag{14}$$

where $\vec{\epsilon}(\vec{q}, \omega)$ is the dielectric tensor of the crystal, $\hat{q}$ is a unit vector in the $\vec{q}$ direction, and $-e$ is the charge on the electron. But it also follows from the definition of the dielectric response function of the crystal that

$$\epsilon(\vec{q},\omega) = 1 - \frac{4\pi}{q^2}\frac{(-e)\delta n(\vec{q},\omega)}{\Phi(q,\omega)}$$

and as a consequence, that

$$\epsilon(\vec{q},\omega) = \hat{q}\cdot\vec{\epsilon}(\vec{q},\omega)\cdot\hat{q} \equiv \epsilon_L(\vec{q},\omega),$$

i.e., the dielectric response function is identical to the longitudinal dielectric function. Here we have assumed, for simplicity, a cubic crystal and a description with respect to principal axes.

It is well established that in the optical limit ($\vec{q}\to 0$) the longitudinal and transverse dielectric functions are equal for cubic crystals.[6] In what follows, collisions are introduced via the relaxation-time approximation and a tacit assumption that the scattering is isotropic. We therefore expect the long-wavelength equality of the transverse and longitudinal dielectric functions to be preserved. Accordingly, for cubic crystals we can extract both the optical behavior and long-wavelength plasma oscillations from the response function $\lim_{q\to 0}\epsilon(\vec{q},\omega) \equiv \epsilon(\omega)$. To obtain the latter we will work in the transverse gauge and consider the response of the crystal to an external charge.

If we identify $\hat{H}_1(\vec{r}, t) = -e\Phi(\vec{r}, t)$, then from Eq. (13)

$$\delta n(\vec{q},\omega) = \frac{1}{\Omega}\sum_{\vec{k}ll'}\frac{f_{\vec{k}+\vec{q},l'} - f_{\vec{k}l}}{\mathcal{E}_{\vec{k}+\vec{q},l'} - \mathcal{E}_{\vec{k}l}}\left|(\vec{k}+\vec{q}l'|\vec{k}l)\right|^2 \times[-e\Phi(\vec{q},\omega) - \delta\mu(\vec{q},\omega)], \tag{15}$$

where

$$(\vec{k}, l|\vec{k}+\vec{q}, l') = \frac{1}{\Omega_a}\int d^3r\, u^*_{\vec{k}l}(r)\, u_{\vec{k}+\vec{q}l'}(\vec{r}).$$

Here Ω_a is the unit cell volume. We see that the net effect of including collisions in a number-conserving fashion via a local chemical potential has been the renormalization of the effective field to which the electrons respond. Rather than responding to $-e\Phi(\vec{q},\omega)$ as in the usual self-consistent field or random-phase approximation, we find that the electrons respond to $-e\Phi(\vec{q},\omega) - \delta\mu(\vec{q},\omega)$.

Adopting a notation similar to that of Mermin's, we now define a quantity $B(\vec{q},\omega)$ by

$$B(\vec{q},\omega) = \frac{1}{\Omega}\sum_{\vec{k}}\sum_{ll'}\frac{f_{\vec{k}+\vec{q}l'} - f_{\vec{k}l}}{\hbar\omega - (\mathcal{E}_{\vec{k}+\vec{q}l'} - \mathcal{E}_{\vec{k}l})}\left|(\vec{k}+\vec{q}l'|\vec{k}l)\right|^2. \tag{16}$$

This is related to the RPA polarizability by

$$4\pi\alpha(\vec{q},\omega) = \lim_{\eta\to 0^+} V_q B(\vec{q},\omega+i\eta), \tag{17}$$

where $V_q = 4\pi e^2/q^2$ is the Fourier transform of the Coulomb potential. Using (16), Eqs. (10) and (8) now give

$$\epsilon(\vec{q},\omega) = 1 - V_q\frac{\delta n(\vec{q},\omega)}{(-e)\Phi(\vec{q},\omega)} = 1 + \frac{V_q B(\vec{q},\omega+i/\tau)}{1-(1-i\omega\tau)^{-1}[1 - B(\vec{q},\omega+i/\tau)/B(\vec{q},0)]}. \tag{18}$$

Taking the limit $\tau\to\infty$, this expression for $\epsilon(\vec{q},\omega)$ reduces precisely to the form for the dielectric response obtained by Ehrenreich and Cohen,[14] namely,

$$\epsilon(\vec{q},\omega) = 1 + \lim_{\eta\to 0^+} V_q B(\vec{q},\omega+i\eta). \tag{19}$$

In expressions of this kind, lifetime effects have previously been introduced by interpreting η, the adiabatic perturbation theory infinitesimal, as a finite inverse relaxation time (i.e., $\eta = 1/\tau$). (The prime on the summation indicates $l \neq l'$ is excluded.)

$$\epsilon(\omega) = \lim_{q\to 0}\epsilon(\vec{q},\omega) = \epsilon_0 - \frac{\omega_{\rm op}^2}{\omega^2} - \frac{4\pi e^2}{m}\int_{\rm BZ}\frac{d^3k}{4\pi^3}\sum_{ll}{}'\frac{f_{\vec{k}l}F^{\mu}_{l'l}}{(\omega+i\eta)^2 - \omega^2_{l'l}}. \tag{20}$$

In this expression, $F^{\mu}_{l'l}$ is the oscillator strength defined by

$$F^{\mu}_{l'l} = \frac{2}{\hbar\omega_{l'l}}\frac{|\langle\vec{k}l'|p^{\mu}|\vec{k}l\rangle|^2}{m},$$

with $p^{\mu} = \hat{q}\cdot\vec{p}$ the momentum operator in the $\hat{q}$ direction and $\hbar\omega_{l'l}$ the energy difference defined by $\hbar\omega_{l'l} = \mathcal{E}_{\vec{k}l'} - \mathcal{E}_{\vec{k}l}$. The conduction-band averaged

("optical") mass m_{op} is then given by

$$1-\frac{m_e}{m_{op}}=\frac{1}{n_c}\int_{BZ}\frac{d^3k}{4\pi^3}\sum_l{}'f_{\vec{k}l}F^{\mu}_{ll_c},$$

where the subscript BZ on the integral indicates its restriction to the first Brillouin zone. By l_c and n_c are meant the conduction band and its electron density, respectively, with m_e the electron mass without band corrections. From this follows the definition of the optical plasma frequency ω_{op}, namely, $\omega_{op}^2=4\pi n_c e^2/m_{op}$. Finally, to complete the explanation of the notation, we note that for both optical and long-wavelength plasma frequencies the core polarization contribution is essentially real. Hence, to simplify matters, we restrict our sums to the valence band and incorporate the effects of core polarization in the constant $\epsilon_0=1+4\pi\alpha_0$, where α_0 is the total core polarizability.

We now compare (20) with the expression (18) for $\epsilon(\omega)$ given by the number-conserving approximation. In a similar notation (18) reads

$$\epsilon(\omega)=\epsilon_0-\frac{\omega_{op}^2}{\omega(\omega+i/\tau)}-\frac{4\pi e^2}{m}(1+i/\omega\tau)\int_{BZ}\frac{d^3k}{4\pi^3}\times\sum_{l,l'}{}'\frac{f_{\vec{k}l}F^{\mu}_{l'l}}{(\omega+i/\tau)^2-\omega^2_{l'l}}. \tag{21}$$

The extraction of the core polarization and the restriction of the sums to the valence bands is still straightforward. It requires noting that

$$\lim_{q\to 0}B(\vec{q},\omega+i/\tau)/B(\vec{q},0)=0,$$

and arguing that the weak frequency dependence of the core contribution due to the $i/\omega\tau$ term is entirely swamped by the leading Drude term. Therefore the difference between (20) and (21) is

$$\Delta\epsilon(\omega)=-\frac{i4\pi e^2}{m}\frac{1}{\omega\tau}\sum_{ll'}{}'\int\frac{d^3k}{4\pi^3}\frac{f_{\vec{k}l}F^{\mu}_{l'l}}{(\omega+i/\tau)^2-\omega^2_{l'l}}. \tag{22}$$

We now examine whether this correction can result in observable effects. As a convenient model system we consider the interband (IB) optical conductivity of aluminum. As discussed in detail in AS, the IB optical conductivity is the sum of parallel band (PB) absorption with its distinctive edge shape, and a broader Wilson-Butcher "normal" IB contribution. In AS, a relatively simple closed-form expression for $\sigma_{PB}(\omega)$ was obtained using (20) and second-order pseudopotential perturbation theory. Within the same approximations it requires little additional effort to obtain $\sigma_{IB}(\omega)$ from the number-conserving expression (21) and the relation $\epsilon(\omega)=1+i4\pi\sigma(\omega)/\omega$. The two results for $\sigma_{IB}(\omega)$ thus obtained are plotted for Al and Na in Figs. 1 and 2. The parameters used for Al are slightly different from those specified in AS. The first two pseudopotential matrix elements used were $V_{111}=0.243$ eV and $V_{200}=0.764$ eV as in Ref. 4; however, to be consistent with the last section of the present paper $V_{220}=1.37$ eV (i.e., the $\vec{K}_{220}$ IB transition) has been included. Furthermore, in order to be consistent with both band calculations and experimental data, a band effective mass $m^*=1.025$ has been used. This value of m^* provides a good fit to the bottom of the band as determined both by numerical band calculations and by analy-

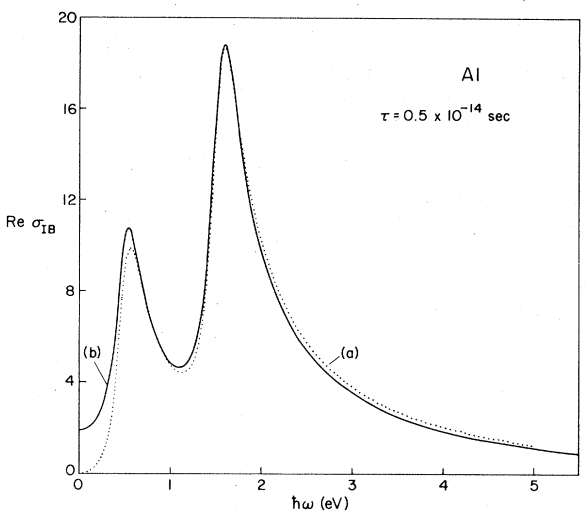

FIG. 1. Optical conductivity for Al for both the Ehrenreich and Philipp (Ref. 1) relaxation-time model (a) and the number-conserving result (b). Note the nonvanishing of $\mathrm{Re}\sigma_{IB}$ at $\omega=0$. Here $\tau=0.5\times10^{-14}$ sec. The unit of conductivity used in these figures is $e^2/24\pi a_0\hbar=5.48\times10^{14}$ sec$^{-1}\equiv1636\ \mu\Omega$ cm.

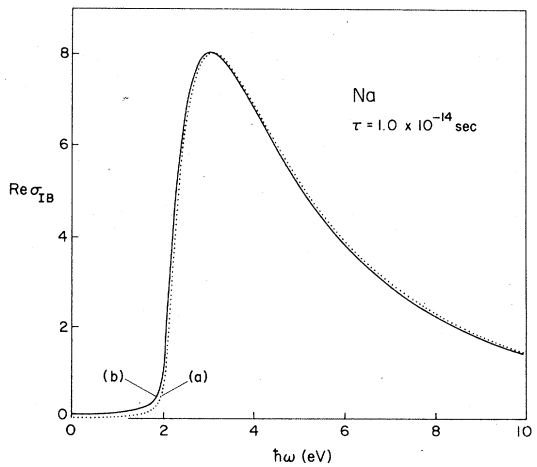

FIG. 2. Same as in Fig. 1 but for Na with $\tau=1.0\times10^{-14}$ sec.

sis of experimental data.[17-19]

The optical mass used in our calculations was computed including the lowest three IB contributions to the conductivity, i.e., the direct transitions corresponding to the reciprocal lattice vectors $\vec{K}_{111}$, $\vec{K}_{200}$, and $\vec{K}_{220}$. This makes our conductivity consistent with the sum rule

$$\int_0^\infty d\omega \, \mathrm{Re}\sigma(\omega) = \omega_p^2/8 \quad (\omega_p^2 = 4\pi n_c e^2/m_e) .$$

However, it should be noted that the inclusion of additional IB transitions will result in an increase in m_{op}. Using the empty-core model for the higher pseudopotential matrix elements, Table I indicates the variation of m_{op} as a function of the number of IB transitions included. Of course any experimentally determined m_{op} must reflect the inclusion of all IB transitions. Nevertheless, since the higher Fourier components of the potential are not accurately known, we have chosen to restrict our calculations to the first three sets of reciprocal-lattice vectors, and we use $m_{op} = 1.61 m_e$.

Upon examination of Figs. 1 and 2 it becomes apparent that except for low frequencies, the corrections introduced by enforcing number conservation are relatively minor for the simple metals. Any experimental optical data that one result purports to fit, the other will also.

The interesting consequence of (21) as applied to $\mathrm{Re}\sigma_{IB}(\omega)$ is the realization that there are IB contributions to the static conductivity i.e., as can be seen in Figs. 1 and 2,

$$\lim_{\omega \to 0} \mathrm{Re}\sigma_{IB}(\omega) \neq 0 .$$

Generally it follows from (21) that

$$\mathrm{Re}\sigma_{IB}(\omega = 0) = \frac{e^2}{\hbar a_0} (v_F \tau) \left(\frac{a_0}{k_F}\right) \times \sum_{ll'}{}' \int_{BZ} \frac{d^3k}{4\pi^3} \frac{f_{\vec{k}l} F^{\mu}_{l'l}}{1 + (\omega_{l'l}\tau)^2} , \qquad (23)$$

where a_0 is the Bohr radius and v_F and k_F are the Fermi velocity and wave vector, respectively. In our relaxation-time approximation approach there is no explicit mechanism for the conversion of IB transitions into Drude-type absorption. However, it must be recognized that the relaxation time represents a description of scattering processes, and hence the strength of the scattering potentials in the metal. As a consequence, the one-electron levels are implicitly both shifted and broadened by the inclusion in the number conserving argument of a local chemical potential which as noted is a function of τ. The nonvanishing of $\mathrm{Re}\sigma_{IB}(\omega = 0)$ is thus a manifestation of the overlapping of the broadened levels. There is a resulting mobility between the corresponding bands that persists to zero frequency. It is of course clear that no such IB contributions to $\mathrm{Re}\sigma_{IB}(\omega)$ can arise from an heuristic introduction of a scattering time by setting $\eta = 1/\tau$ as in Eq. (20). This follows immediately from the role that the infinitesimal plays in adiabatic perturbation theory: it is the infinitely slow rate by which the *external* perturbation is introduced to the system so as to ensure that there are no shifts in the energy levels. In contrast, in the relaxation-time theory developed here, the scattering time τ is an intrinsic property of the system, and it is the number conservation requirement that implies a local chemical potential which can shift the single-particle energies. Thus the introduction of $\delta\mu(\vec{r}, t, \tau)$ via a conserving approximation is necessary to effect a shift of the energy levels.

Such contributions at small ω from interband processes have in fact been discussed by others. In particular, Nettel[20] and Stevenson[21] have observed that optical absorption aided by 1-phonon processes can lead to indirect interband transitions. As in our case, the resultant interband absorption then begins well below the onset of the usual (direct) IB processes. Quite recently, Chakraborty and Allen have arrived independently at the conclusion that in the presence of an electronic scattering mechanism (such as disorder), IB transitions do indeed contribute to the dc conductivity.[22] While their approach via semiclassical transport theory[23,24] includes higher-order contributions neglected in our relaxation-time approach, nevertheless, their resultant formalism does not readily lend itself to the straightforward numerical evaluation that our phenomenological relaxation-time equation permits.

We arrive, however, at a conclusion similar to that of Chakraborty and Allen[22] as to the existence of a "saturation" conductivity. In Fig. 3 a plot of $\mathrm{Re}\sigma_{IB}(0)$ is provided for Al as a function of the logarithm of the scattering time τ. As might be expected, both the limits $\lim_{\tau \to \infty} \mathrm{Re}\sigma_{IB}(0)$ and $\lim_{\tau \to 0} \mathrm{Re}\sigma_{IB}(0)$ are found to vanish. However, the taking of the latter limit is both unwarranted and

TABLE I. Optical mass as a function of the number of IB transitions included. Results for Al and Na.

Al IB transitions included	m_{op}/m_e	Na IB transitions included	m_{op}/m_e
{111}	1.11	{110}	1.02
{200}	1.57	{200}	1.02
{220}	1.61	{211}	1.03
{311}	1.64	{220}	1.03
{222}	1.65		
{400}	1.65		

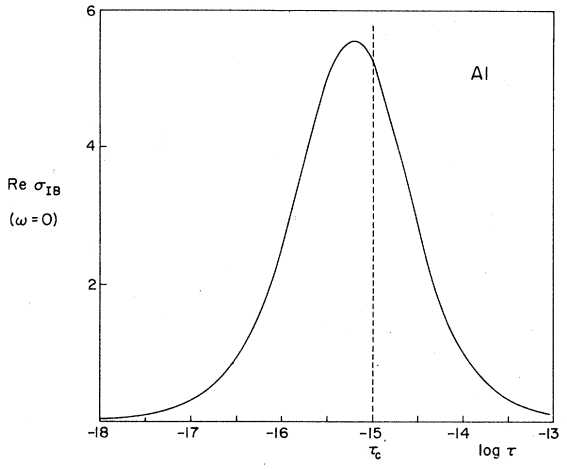

FIG. 3. Plot of Eq. (23) as applied to Al. As discussed in the text an approximate cutoff relaxation time is indicated. (Vertical dashed line.) The relaxation-time approximation is meaningful for scattering times larger than this cutoff.

unphysical, since clearly our model cannot be meaningful when $v_F\tau$, the mean path length at the Fermi surface, is on the order of a lattice spacing. When this occurs, multiple scattering events make a more rigorous approach necessary. It is for this reason that a rough cutoff scattering time τ_c is indicated in Fig. 3. The choice of $\tau_c = 1.0\times10^{-15}$ sec corresponds in Al to a mean free path $v_F\tau$ at the Fermi surface of about five lattice spacings. For shorter scattering times the relaxation-time approximation becomes quite dubious.

The conductivity at this cutoff corresponds to the notion of saturation of Chakraborty and Allen. If, in fact, very strong electronic localization does *not* occur as the disorder increases, but a Boltzmann or Liouville single scattering transport equation does indeed remain valid, then the IB contributions result in a minimum in the dc conductivity, or a maximum (saturation) in the resistivity.

The contribution of $\mathrm{Re}\sigma_{IB}(0)$ in the simple metals is very small. Experimentally, the relaxation-time range in Al is observed to be about 0.2–0.5 $\times10^{-14}$ sec for temperatures between 198 and 552°K.[25] But for $\tau = 0.5\times10^{-14}$ sec, $\mathrm{Re}\sigma_{IB}(\omega) = 1.9e^2/24\pi\hbar a_0$, whereas $\sigma_{\mathrm{Drude}} = 400e^2/24\pi\hbar a_0$; i.e., the IB contribution is only 0.5% of the total dc conductivity. Even at our imposed relaxation-time cutoff of 1.0×10^{-15} sec, $\mathrm{Re}\sigma_{IB}(0)/\sigma_{\mathrm{Drude}}$ is only 0.15. It follows that the IB contribution to the dc conductivity is experimentally undetectable or inseparable from the Drude term in the simple metals. Nevertheless, systems in which $\mathrm{Re}\sigma_{IB}(0)$ is non-negligible are imaginable, and as Chakraborty and Allen have pointed out, if the oscillator strengths in (21) are sufficiently strong, then sum-rule considerations imply a reduction in σ_{Drude}. The result would be a significant portion of the dc conductivity arising from $\mathrm{Re}\sigma_{IB}(0)$. We are presently examining the consequences of this possibility.

IV. CONTRIBUTION OF THE LOCAL FIELD

In Sec. III we derived the dielectric response of a crystal by working entirely with macroscopic quantities. Macroscopic quantities, in the present context, are those whose spatial variations are small on the scale of a unit cell. Equivalently, we may describe them as quantities whose largest significant Fourier component lies in the first Brillouin zone.

Not all of the quantities involved in obtaining the solution for $\epsilon(\vec{q},\omega)$ are macroscopic in this sense. As an example, even though the external electromagnetic field is slowly varying, the response to it of the charge in the immediate vicinity of an ion core or a surface can be very rapid. This local response will involve Fourier components outside the first Brillouin zone. We can then expect similar behavior of the self-consistent field within the crystal. In particular, the bulk response of a crystal to an external field $\vec{E}^{\,\mathrm{ext}}(\vec{q},\omega)$ will, on the microscopic level, involve Bragg-diffracted Fourier components such as $\vec{E}^{\,\mathrm{mic}}(\vec{q}+\vec{K},\omega)$, where $\vec{K}$ is a reciprocal-lattice vector.

To average these quantities before calculating $\epsilon(\vec{q},\omega)$, as is done in Sec. III, is not strictly the proper procedure, though it is often a plausible approximation. It would seem easiest, of course, to deal directly with the macroscopic external pertrubation in calculating the response of the system. Ehrenreich[16] has outlined the general method for achieving this aim, but his prescription cannot be followed in the single-particle self-consistent field approach. The correct averaging procedure to calculate the macroscopic $\epsilon(\vec{q},\omega)$ within the context of the self-consistent RPA has been developed by Adler,[6] Wiser,[5] and again later by Ehrenreich.[16] Both Adler and Wiser have argued that the local-field corrections to $\epsilon(\vec{q},\omega)$ stemming from a proper averaging are small in simple metals. (Once again, by simple metal, we mean one with a nearly-free-electron band structure and a tightly bound core.)

More recent calculations suggest that local-field effects are of importance in explaining optical data in covalently bonded solids,[26-28] as well as plasmon line shapes in metals and semiconductors.[7] With this in mind, we present here an analysis of the local-field contribution to the optical properties of aluminum in the long-wavelength limit carried out within the number-conserving approxima-

tion. As predicted, the correction will be small; nevertheless, features of the local-field corrections that one might expect to be generalizable to other systems will be found.

We first provide the general relaxation-time result for the macroscopically averaged dielectric function. Though adapted to Mermin's conserving approximation, the procedure followed is equivalent to that used by Wiser. The result presented here is analogous to Wiser's Eq. (34):

$$\epsilon(\vec{q},\omega)=[(\vec{\epsilon}^{-1})_{0,0}]^{-1}=\epsilon_{0,0}(\vec{q},\omega)+\sum_{\vec{K}\neq 0}\epsilon_{0\vec{K}}\frac{(\vec{\epsilon})^{\vec{K},0}}{(\vec{\epsilon})^{0,0}}. \tag{24}$$

Here superscripts denote the indicated cofactor. The matrix elements of the dielectric matrix $\epsilon_{\vec{K}\vec{K}'}(\vec{q},\omega)$ are defined by

$$\epsilon_{\vec{K}\vec{K}'}(\vec{q},\omega)=\delta_{\vec{K}\vec{K}'}+\frac{4\pi e^2}{(\vec{q}+\vec{K})^2}\sum_{\vec{Q}}\left\{\vec{1}+\frac{1}{1-i\omega\tau}\left[\vec{B}(\vec{q},\omega+i/\tau)\vec{B}^{-1}(\vec{q},0)-\vec{1}\right]\right\}^{-1}_{\vec{K},\vec{Q}}B_{\vec{Q},\vec{K}'}(\vec{q},\omega+i/\tau). \tag{25}$$

In turn, the matrix elements of $\vec{B}(\vec{q},\omega)$ are given by

$$B_{\vec{K}\vec{K}'}(\vec{q},\omega)=\frac{1}{\Omega}\sum_{\vec{k}ll'}\frac{f_{\vec{k}+\vec{q}l'}-f_{\vec{k}l}}{\hbar\omega-(\mathcal{E}_{\vec{k}+\vec{q}l'}-\mathcal{E}_{\vec{k}l})}(\vec{k}l|e^{-i\vec{K}\cdot\vec{r}}|\vec{k}+\vec{q}l')(\vec{k}+\vec{q}l'|e^{i\vec{K}'\cdot\vec{r}}|\vec{k}l).$$

In this notation, the dielectric function of Sec. III is written $\epsilon_{0,0}(\vec{q},\omega)$. (Note: $1/\tau$ here is the relaxation rate, not the more conventional infinitesimal quantity.)

As in Sec. III, we now specialize to the case of a simple metal, or more generally, to a solid described by a weak pseudopotential. Using (24), $\epsilon(\omega)=\epsilon(\vec{q}\to 0,\omega)$ is expressible to second order in the pseudopotential matrix elements $V_{\vec{K}}$. Again, the result is not dissimilar from Wiser's. The total macroscopically averaged optical response function appears as

$$\epsilon(\omega)=\lim_{q\to 0}\left\{1+\frac{4\pi e^2}{q^2}(1+i/\omega\tau)B_{0,0}(\vec{q},\omega+i/\tau)-\frac{4\pi e^2}{q^2}\sum_{\vec{K}\neq 0}\frac{B_{\vec{K}0}(\vec{q},\omega+i/\tau)B_{0\vec{K}}(\vec{q},\omega+i/\tau)}{\Delta_{\vec{K}\vec{K}}(\vec{q},\omega+i/\tau)}\left[\frac{4\pi e^2}{K^2}+\frac{i}{\omega\tau}\left(\frac{4\pi e^2}{K^2}+\frac{1}{B_{\vec{K}\vec{K}}(\vec{q},0)}\right)\right]\right\}, \tag{26}$$

where

$$\Delta_{\vec{K}\vec{K}}(\vec{q},\omega)=1+\frac{1}{1-i\omega\tau}\left(\frac{B_{\vec{K}\vec{K}}(\vec{q},\omega)}{B_{\vec{K}\vec{K}}(\vec{q},0)}-1\right)+\frac{4\pi e^2}{K^2}B_{\vec{K}\vec{K}}(\vec{q},\omega).$$

In the nearly-free-electron approximation the local-field (LF) contribution for a cubic crystal can be re-expressed as

$$\epsilon^{\mathrm{LF}}(\omega)=-\frac{1}{3}\sum_{\vec{K}\neq 0}\frac{\frac{[\mathfrak{B}_{0\vec{K}}(\omega+i/\tau)]^2}{(2\pi a_0K)^2}\left[1+\frac{i}{\omega\tau}\left(1+\frac{\pi a_0K}{2b_{\vec{K}\vec{K}}}\right)\right]}{1+\frac{1}{1-i\omega\tau}[\mathfrak{B}_{\vec{K}\vec{K}}(\omega+i/\tau)/b_{\vec{K}\vec{K}}-1]+\frac{2}{\pi a_0K}\mathfrak{B}_{\vec{K}\vec{K}}(\omega+i/\tau)}. \tag{27}$$

The reduced matrix elements here are defined by

$$\mathfrak{B}_{0\vec{K}}(\omega)=\frac{K^3}{2}\left(\frac{4\pi e^2}{K^2}\right)^2(a_0K)^2\times\int\frac{d^3k}{4\pi^3}f_{\vec{k}}\frac{1}{(1+x^2)^{1/2}}\frac{1}{(\hbar\omega)^2-4V_K^2(1+x^2)},$$

$$\mathfrak{B}_{\vec{K}\vec{K}}(\omega)=-2\pi(a_0K)\left(\frac{4\pi e^2}{K^2}\right)V_{\vec{K}}\times\int\frac{d^3k}{4\pi^3}f_{\vec{k}}\frac{(1+x^2)^{1/2}}{(\hbar\omega)^2-4V_K^2(1+x^2)}, \tag{28}$$

and

$$b_{\vec{K}\vec{K}}=\frac{\pi}{2}(a_0K)\left(\frac{4\pi e^2}{K^2}\right)\frac{1}{V_{\vec{K}}}\int\frac{d^3k}{4\pi^3}f_{\vec{k}}\frac{1}{(1+x^2)^{1/2}},$$

where

$$x=\frac{\mathcal{E}_K}{2|V_K|}(1-2\vec{k}\cdot\vec{K}/K^2).$$

Note that the integrals and occupation factors are extended over all $\vec{k}$ space. As in the paper by Ashcroft and Sturm, a 2-PW approximation has been made. The integrals can be evaluated in a straightforward fashion following their procedure. Some care must be taken, however, in the selection of integral limits in order to distinguish the parallel band contribution from the Wilson-Butcher contribution. These limits are functions of both the reciprocal-lattice vector $\vec{K}$ under consideration, and the Fermi energy. Closed-form expressions for these reduced matrix elements are provided in the Appendix.

In Figs. 4 and 5 we display the LF contribution to the optical conductivity, $\mathrm{Re}\sigma_{\mathrm{LF}}(\omega)$, in Al and Na

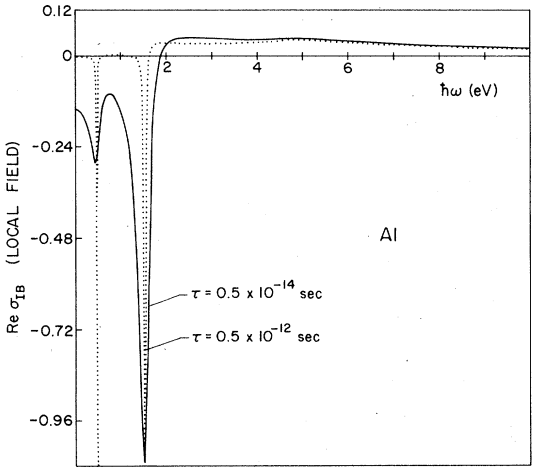

FIG. 4. Plots of the local-field contribution to the optical conductivity in Al for scattering times $\tau = 0.5 \times 10^{-12}$ sec (dotted) and 0.5×10^{-14} sec (full line). The edges correspond to IB transitions. For $\tau = 0.5 \times 10^{-12}$ sec the minima are off-scale at -16.5 and -80.8, respectively.

as a function of relaxation time. Although the contribution is small, since the structure exhibited is determined by the nature of the available IB transitions, we can expect the results to be generalizable. For both Al and Na, $\mathrm{Re}\sigma_{\mathrm{LF}}(\omega)$ has its (negative) minima in the frequency range where $\mathrm{Re}\sigma_{\mathrm{IB}}(\omega)$ is peaking. $\mathrm{Re}\sigma_{\mathrm{LF}}(\omega)$ for Na has the same broad form as the Wilson-Butcher $\mathrm{Re}\sigma_{\mathrm{IB}}(\omega)$ curve (Fig. 2), although reflected through the abscissa.

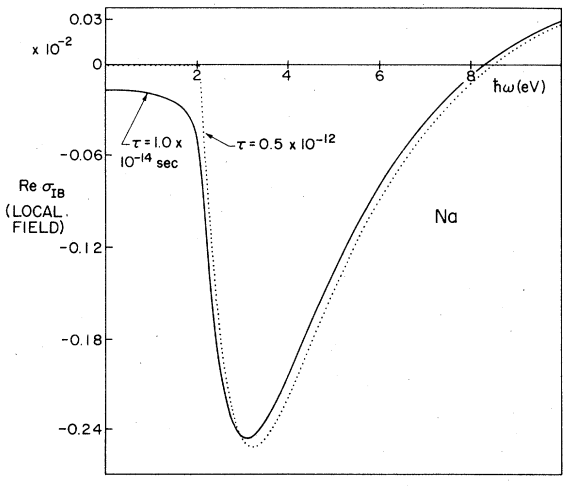

FIG. 5. Plots of the local-field contribution to the optical conductivity in Na for scattering times of 0.5×10^{-12} sec (dotted) and 1.0×10^{-4} sec (full curve). Note the contrast to Fig. 4 for Al: For Na a Butcher-Wilson-type shape is found and is lacking the characteristic edge structure of the polyvalent metals.

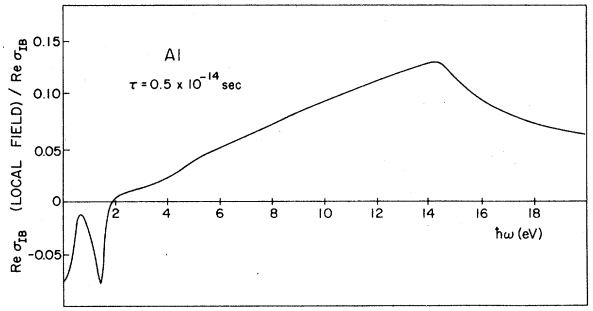

FIG. 6. Fractional changes in the optical conductivity of Al arising from local-field corrections in the optical range ($\tau = 0.5 \times 10^{-14}$ sec).

The lack of structure is due to the complete containment of the Fermi surface within the first BZ. By contrast, we see in Al that $\mathrm{Re}\sigma_{\mathrm{LF}}(\omega)$ has sharp edges at the two IB energies corresponding to the PB optical absorption of $\mathrm{Re}\sigma_{\mathrm{IB}}(\omega)$. This results from the segments of the Fermi surface of Al which penetrate the second BZ. The net effect of including the LF in a calculation is therefore a broadening of the edge shape and a decrease of the IB absorption maxima in $\mathrm{Re}\sigma(\omega)$ as compared to $\mathrm{Re}\sigma_{0,0}(\omega)$. In Fig. 6 we see that for Al in the optical range $0 \leq \hbar\omega \leq 20$ eV, the local-field term var-

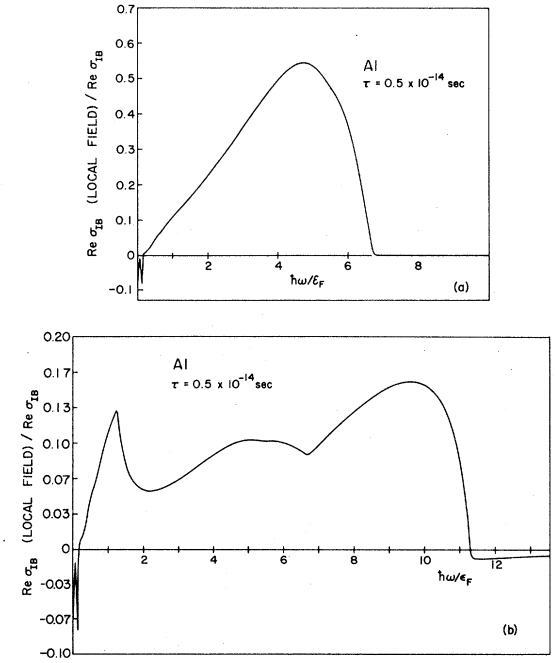

FIG. 7. Same as Fig. 6, but now the energy range has been increased up to about 100 eV. The difference in scales demonstrates the necessity of including higher IB transitions in a calculation of the local field ($\tau = 0.5 \times 10^{-14}$ sec). In (a), K_{111} and K_{200} are included. In (b) K_{220} is included as well.

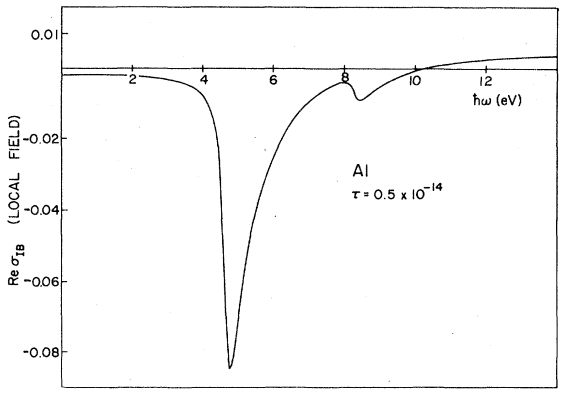

FIG. 8. Plot of a 1-PW calculation of the local field in Al. The structure is now similar to that of Fig. 5 for Na. All IB structure has been washed out ($\tau = 0.5 \times 10^{-14}$ sec). Here $m^* = 1.0$ for comparison with the work of others ($m^* = 1.025$ leads to no significant change).

ies as a correction to the IB absorption between -7% and 14%. Finally, we note from Figs. 4 and 5 that as the scattering rate is increased the LF response is broadened with a decrease of the IB edges.

As would be expected, for higher energies the inclusion of correspondingly higher IB transitions is necessary in order to calculate the correct LF contribution. Figure 7 confirms this in plots of the ratio of the LF correction to normal IB absorption in the range $0 \leq \hbar\omega \leq 7\mathcal{E}_F$; curve 7(a) includes K_{111} and K_{200}; curve 7(b) includes K_{220} as well.

Finally, in Fig. 8 the results of a 1-PW LF calculation are plotted in order to make comparison with our 2-PW result for Al. Agreement in the visible optical range is not to be expected, and the differences are both significant and predictable. The 1-PW minima correspond to Butcher-Wilson IB absorption maxima just as in the 2-PW model the minima corresponded to PB absorption onset. Furthermore, the 2-PW model gives an LF contribution to Reσ three times as large as the 1-PW result in the range $10 \leq \hbar\omega \leq 20$ eV. The narrow PB absorption, as opposed to the broad Butcher-Wilson absorption, spreads the LF contribution over a larger energy range. For the same sum-rule considerations as in the optical case, we can expect difficulties in approximating the LF contribution to the energy-loss function $\mathrm{Im}[-1/\epsilon(\vec{q}, \omega)]$ with a 1-PW model even at $\hbar\omega_p$. These differences between a 1-PW and 2-PW calculation should be borne in mind when considering Sturm's 1-PW LF corrections to plasmon line widths[7] and his demonstration of the "equivalence" of the LF and dynamic screening.[29] In particular, such equivalence does not hold for polyvalent metals in the optical region where it is crucial to include the effects of zone degeneracy both on $\epsilon_{0,0}(\vec{q}, \omega)$ and on the LF contribution.

V. PLASMON DISPERSION AND DAMPING

It has been demonstrated by a number of authors[8-12,30] that the dominant plasmon decay channel in metals is interband (IB) transitions. In particular, the series of papers by Sturm demonstrates that a 1-PW model for a nearly free electron moving in a weak pseudopotential is sufficient for a good quantitative understanding of the effect of IB transitions on the plasma frequency and damping in simple metals. Prior to the realization of the importance of the periodic nature of the crystal potential in determining the behavior of electronic plasma, attempts were made to fit electron-loss experimental data with various dielectric functions[31,32] for the homogeneous electron gas. These approaches attempted to fit the observed line widths with overly large scattering times—scattering times that subsumed the then unrecognized damping due to IB transitions. As a result, consistent agreement with experimental results was not found. While it is true that the primary contribution to plasmon decay is IB transitions, the calculated full width at half maxima due to IB damping alone in the simple metals are about 0.1 eV smaller than the accepted experimental values. In the number-conserving relaxation-time approximation the additional broadening is successfully accounted for phenomenologically by the inclusion of a scattering time.

The importance of IB transitions can be readily understood. As an example, consider the decay of the long wavelength ($\vec{q} = 0$) 15.0 eV plasmon in Al. In a translationally invariant electron gas the simultaneous requirements of energy and momentum conservation prevent its possible decay into an electron-hole pair. By contrast, in a periodic system it is crystal momentum that must be conserved. For example, in an extended zone scheme, the energy necessary to create a hole near the Fermi surface by the IB transition $k_F \rightarrow k_F - K_{220}$ is $\mathcal{E}^0_{k_F - K_{220}} - \mathcal{E}^0_{k_F} = 14.88$ eV. (Here $\mathcal{E}^0_k = \hbar^2 k^2/2m$.) Such a transition is thus a means of decay for the $q = 0$ plasmon. In aluminum IB transitions for all reciprocal-lattice vectors less than or equal to K_{220} contribute to such decay; larger ones do not. As a consequence of IB decay, $\mathrm{Im}\epsilon(\vec{q}, \omega)$ and hence the plasmon damping are nonvanishing even in the collisionless regime.[32] However, as indicated above, IB transitions do not account for all the plasmon decay channels in a solid. Though of lesser strength, other electron scattering mechanisms do exist. In the relaxation time approximation this further degradation is parametrized by the scattering time τ.

TABLE II. Plasmon energy, damping, and FWHM for Al as a function of scattering time. Here $m^*=1.025m_e$, $m_{op}=1.61m_e$, $\epsilon_b=1.04$, $V_{111}=0.243$ eV, $V_{200}=0.764$ eV, and $V_{220}=1.370$ eV. The value of the plasmon energy cited, $\hbar\omega_p(0)$, is that for which the energy-loss function has its maximum value at $q=0$.

τ (sec)	$\hbar\omega_p(0)$ (eV)[a]	FWHM(τ) (eV)[b]	$2\gamma_p(\tau)$ (eV)[c]	$2\Gamma(\tau)$ (eV)[d]
0.5×10^{-12}	15.12	0.39	0.346	0.345
1.0×10^{-13}	15.12	0.40	0.356	0.350
0.5×10^{-13}	15.12	0.40	0.369	0.357
1.0×10^{-14}	15.12	0.46	0.472	0.410
0.9×10^{-14}	15.12	0.46	0.487	0.418
0.7×10^{-14}	15.12	0.48	0.528	0.439
0.5×10^{-14}	15.13	0.52	0.602	0.478
0.3×10^{-14}	15.13	0.61	0.775	0.567
1.0×10^{-15}	15.14	1.06	1.65	1.02

[a] Plasmon energy is calculated by maximizing the energy-loss function including the local field.

[b] The FWHM including the local field from Eq. (29). Verification of Matthiessen's law is immediate.

[c] The damping calculated by Eq. (40); the local field is *not* included.

[d] The FWHM as calculated from Eq. (29); to make comparison with $\gamma_p(\tau)$ the local field is excluded here.

Within the framework of the collisionless RPA, the line shape of the electron energy-loss function $\mathrm{Im}[-1/\epsilon(\vec{q},\omega)]$ is expected to be Lorentzian. As a result, the FWHM is twice the damping Γ—the imaginary part of the plasmon frequency. Both are given by[33]

$$\Gamma=\left.\frac{\mathrm{Im}\epsilon(\vec{q},\omega)}{\left(\frac{\partial}{\partial\omega}\,\mathrm{Re}\epsilon(\vec{q},\omega)\right)}\right|_{\omega=\omega_p}. \tag{29}$$

It is readily shown[8] that so long as $\mathrm{Re}\epsilon(\omega_p)\approx0$ and $\mathrm{Im}\epsilon(\omega_p)$ is slowly varying, Eq. (28) is always the expression for the FWHM irrespective of the derivation of $\epsilon(\vec{q},\omega)$. As a result, although we will find that the number conserving RPA with collisions developed here gives a different expression for the damping, the full width at half maximum as a function of scattering time will continue to be given by $\mathrm{FWHM}(\tau)=2\Gamma(\tau)$. We will continue to define $\Gamma(\tau)$ by (29), but it is no longer the imaginary part of the plasmon frequency. Furthermore, we are led to an approximate Matthiessen's rule between the inverse scattering time $1/\tau$ and the collisionless damping which arises from IB transitions alone. Thus, direct calculations of the FWHM(τ) for Al and Na shown in Tables II and III as a function of τ justify writing:

$$\mathrm{FWHM}(\tau)=\hbar/\tau+\mathrm{FWHM}(\tau=\infty).$$

We now proceed to derive the plasmon dispersion relationship in the number-conserving relaxation-time approximation. The procedure is that used by others in describing classical plasma oscillations and exploits the similarity between the quantum-mechanical Liouville equation and the Boltzmann equation.[16,34] We regard the plasmon as a self-sustaining charge distribution $-e\delta n(\vec{r},t)$. The corresponding potential $\Phi(\vec{r},t)$ satisfies Poisson's

TABLE III. Plasmon energy, damping, and FWHM for Na as a function of scattering time. Here $m^*=1.00m_e$, $m_{op}=1.02m_e$, and $V_{110}=0.26$ eV. Superscripts a–d have the same meaning as in Table II.

τ (sec)	$\hbar\omega_p(0)$ (eV)[a]	FWHM(τ) (eV)[b]	$2\gamma_p(\tau)$ (eV)[c]	$2\Gamma(\tau)$ (eV)[d]
0.5×10^{-12}	5.86	0.107	0.112	0.111
1.0×10^{-13}	5.86	0.112	0.123	0.116
0.5×10^{-13}	5.86	0.119	0.136	0.123
1.0×10^{-14}	5.86	0.172	0.238	0.175
0.9×10^{-14}	5.86	0.179	0.253	0.182
0.7	5.86	0.200	0.293	0.203
0.5	5.86	0.237	0.367	0.241
0.3	5.85	0.325	0.541	0.328
0.1	5.84	0.774	1.471	0.774

equation:

$$\nabla^2\Phi(\vec{r},t)=4\pi e\,\delta n(\vec{r},t)\,.$$

In the notation of the previous sections, the interaction energy is

$$H_1(\vec{q},\vec{K},\omega)=-e\Phi(\vec{q},\vec{K},\omega)=\frac{4\pi e^2}{(\vec{q}+\vec{K})^2}\,\delta n(\vec{q},\vec{K},\omega)\,. \tag{30}$$

Furthermore, it is not hard to show that

$$\delta n(\vec{q},\vec{K},\omega)=-\sum_{\vec{G}}B^{-1}_{\vec{K}\vec{G}}(\vec{q},0)[H_1(\vec{q},\vec{G},\omega)-\delta\mu(\vec{q},\vec{G},\omega)]\,, \tag{31}$$

where by definition

$$\begin{aligned}\delta n(\vec{q},\vec{K},\omega)&=\mathrm{Tr}\rho^{(1)}e^{-i(\vec{q}+\vec{K})\cdot\vec{r}}\\&=\sum_{\vec{k}ll'}\langle\vec{k}+\vec{q}l'|\rho^{(1)}|\vec{k}l\rangle\,\eta^*_{\vec{k}}\,,\\ \eta_{\vec{k}}&=\langle\vec{k}l|e^{-i(\vec{q}+\vec{K})\cdot\vec{r}}|\vec{k}+\vec{q}l'\rangle\,.\end{aligned} \tag{32}$$

Combining Eqs. (30), (31), and (32) we find

$$\begin{aligned}\langle\vec{k}+\vec{q}l'|\rho^{(1)}|\vec{k}l\rangle&=\frac{-(f_{\vec{k}+\vec{q}l'}-f_{\vec{k}l})}{\hbar(\omega+i/\tau)-(\mathcal{E}_{\vec{k}+\vec{q}l'}-\mathcal{E}_{\vec{k}l})}\left(\langle\vec{k}+\vec{q}l'|\hat{H}_1|\vec{k}l\rangle-\frac{i\hbar/\tau}{\mathcal{E}_{\vec{k}+\vec{q}l'}-\mathcal{E}_{\vec{k}l}}\langle\vec{k}+\vec{q}l'|\hat{H}_1-\delta\hat{\mu}\,|\vec{k}l\rangle\right)\\&=\frac{-(f_{\vec{k}+\vec{q}l'}-f_{\vec{k}l})}{\hbar(\omega+i/\tau)-(\mathcal{E}_{\vec{k}+\vec{q}l'}-\mathcal{E}_{\vec{k}l})}\;\frac{1}{\Omega}\sum_{\vec{K}}\left(\frac{4\pi e^2}{(\vec{q}+\vec{K})^2}\,\eta^*_{\vec{K}}+\frac{i\hbar/\tau}{\mathcal{E}_{\vec{k}+\vec{q}l}-\mathcal{E}_{\vec{k}l}}\sum_{\vec{G}}B^{-1}_{\vec{G}\vec{K}}(\vec{q},0)\eta^*_{\vec{G}}\right)\delta n(\vec{q},\vec{K},\omega)\,,\end{aligned} \tag{33}$$

where the additional relationships

$$\begin{aligned}\langle\vec{k}+\vec{q}l'|\hat{H}_1-\delta\mu\,|\vec{k}l\rangle&=\frac{1}{\Omega}\sum_{\vec{G}}[H_1(\vec{q},\vec{G},\omega)-\delta\mu(\vec{q},\vec{G},\omega)]\eta^*_{\vec{G}}\\&=\frac{-1}{\Omega}\sum_{\vec{G}}\sum_{\vec{K}}B^{-1}_{\vec{G}\vec{K}}(\vec{q},0)\times\delta n(\vec{q},\vec{K},\omega)\eta^*_{\vec{G}}\end{aligned} \tag{34}$$

and

$$\langle\vec{k}+\vec{q}l'|\hat{H}_1|\vec{k}l\rangle=\frac{1}{\Omega}\sum_{\vec{K}}\frac{4\pi e^2}{(\vec{q}+\vec{K})^2}\,\delta n(\vec{q},\vec{K},\omega)\,\eta^*_{\vec{K}} \tag{35}$$

have been used.

Now returning to (33) and summing both sides of the equation over $\vec{k}$, l, and l', we arrive at

$$\begin{aligned}1=-\sum_{\vec{k}ll'}&\frac{f_{\vec{k}+\vec{q}l'}-f_{\vec{k}l}}{\hbar(\omega+i/\tau)-(\mathcal{E}_{\vec{k}+\vec{q}l'}-\mathcal{E}_{\vec{k}l})}\\&\times\frac{1}{\Omega}\sum_{\vec{K}}\left(\frac{4\pi e^2}{(\vec{q}+\vec{K})^2}\,\eta^*_{\vec{K}}\eta_{\vec{K}}+\frac{i\hbar/\tau}{\mathcal{E}_{\vec{k}+\vec{q}l'}-\mathcal{E}_{\vec{k}l}}\times\sum_{\vec{G}}B^{-1}_{\vec{G}\vec{K}}(\vec{q},0)\eta^*_{\vec{G}}\eta_{\vec{K}}\right).\end{aligned} \tag{36}$$

This is the number-conserving relaxation-time approximation plasmon dispersion relationship. The result becomes more manageable if we neglect the contribution of the local field. In this case (36) becomes

$$\begin{aligned}1=-\frac{V_q}{\Omega}\sum_{\vec{k}ll'}&\frac{(f_{\vec{k}+\vec{q}l'}-f_{\vec{k}l})|\langle\vec{k}+\vec{q}l'|\vec{k}l\rangle|^2}{\hbar(\omega+i/\tau)-(\mathcal{E}_{\vec{k}+\vec{q}l'}-\mathcal{E}_{\vec{k}l})}\\&\times\left(1+\frac{i\hbar/\tau}{\mathcal{E}_{\vec{k}+\vec{q}l'}-\mathcal{E}_{\vec{k}l}}\;\frac{1}{4\pi\alpha(\vec{q},0)}\right)\end{aligned} \tag{37}$$

[where $\alpha(\vec{q},0)$ is the RPA polarizability]. Finally, in the $q\to 0$ limit Eq. (36) can be written as

$$1=-V_q B(\vec{q},\omega+i/\tau)\,. \tag{38}$$

Furthermore, in the collisionless limit ($\tau\to\infty$) we recover the standard RPA result for the plasmon dispersion:

$$1=-4\pi\alpha(\vec{q},\omega)\,. \tag{39}$$

Contact between this collisionless relation (39) and the dispersion relationship (38) can also be made in the $\tau\to\infty$ limit via the identity (17). That there is a difference in the dispersion relations with and without collisions is not surprising. It is somewhat analogous to the difference between the normal mode and ringing frequencies of a damped harmonic oscillator: In the absence of collisions the plasmon normal mode frequency is determined by the RPA condition (39), whereas if frictional forces are included the system rings at a shifted frequency. Moreover, in our case there is a factor in competition with the "frictional" damping in determining the plasma frequency: The broadening of the energy levels makes possible a larger Drude-type contribution acceleration of the electrons. This might tend to shift the resonance frequency to higher energy as opposed to a downward shift due to damping. For the purposes of this analysis we have taken the maximum of the energy-loss function to be the plasmon energy. Its values prove to be only a weak function of the scattering time as shown in Tables II and III. Use of Eq. (37) results in no significant numerical difference for the plasmon energy from the values cited in Tables II and III.

As mentioned above, there is also a corresponding change in the result for plasmon lifetime or damping. In the case of simple metals and in the

long-wavelength limit, it is sufficient to work with Eq. (38). Writing the complex plasma frequency as $\omega_p(\vec{q}) = \omega_p^r(\vec{q}) - i\gamma_p(\vec{q})$, assuming that $\gamma_p \ll \omega_p$, and decomposing $B(\vec{q}, \omega)$ into its real and imaginary parts $B_1(\vec{q}, \omega) + iB_2(\vec{q}, \omega)$, one obtains

$$\gamma_p = \frac{B_2(\vec{q}, \omega_p^r(\vec{q}))}{\left(\frac{\partial}{\partial\omega} B_1(\vec{q}, \omega)\right)\Big|_{\omega=\omega_p^r(\vec{q})}} . \tag{40}$$

Written in terms of the number conserving dielectric function, Eq. (40) becomes at $\vec{q} = 0$:

$$\gamma_p = \frac{\mathrm{Im}\left(\frac{\omega_p^r}{\omega_p^r + i/\tau}\,[\epsilon(\omega_p^r) - 1]\right)}{\frac{\partial}{\partial\omega}\left(\mathrm{Re}\,\frac{\omega}{\omega + i/\tau}\,[\epsilon(\omega) - 1]\right)\Big|_{\omega=\omega_p^r(\vec{q})}} . \tag{41}$$

In the simple metals we find that $\gamma_p(\tau) \gtrsim \Gamma(\tau)$. The difference between the damping $\gamma_p(\tau)$ and the full width at half maximum has the same root as the IB contribution to the dc conductivity. As a result of the implicit introduction of a scattering potential via the scattering time τ, the energy levels have been broadened, thereby narrowing the IB gap. This leads to easier decay of the plasmon through IB excitation of electron-hole pairs. Thus in the number-conserving relaxation-time approximation the IB and electronic scattering decay channels for the plasmon are *not* independent. As a result, we emphasize that the above quoted Matthiessen's rule is only a rule of thumb and not theoretically justifiable.

In Figs. 9 and 10 we illustrate the calculated dependence of the energy-loss functions of Al and Na on the scattering time. The calculations presented for Al in Fig. 9 used a band effective mass of

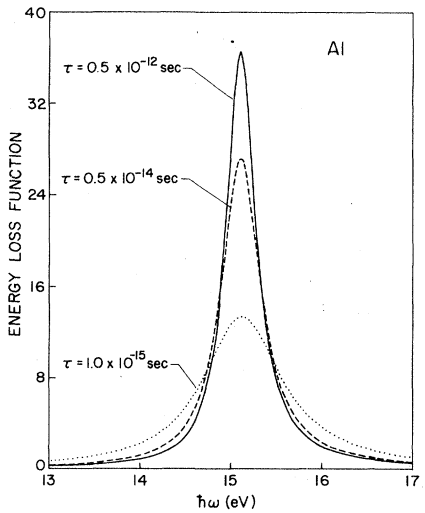

FIG. 9. Plots of the energy-loss function for Al for various scattering times. The parameters used are $\epsilon_0 = 1.04$, $m_{op} = 1.61\, m_e$, and $m^* = 1.025\, m_e$.

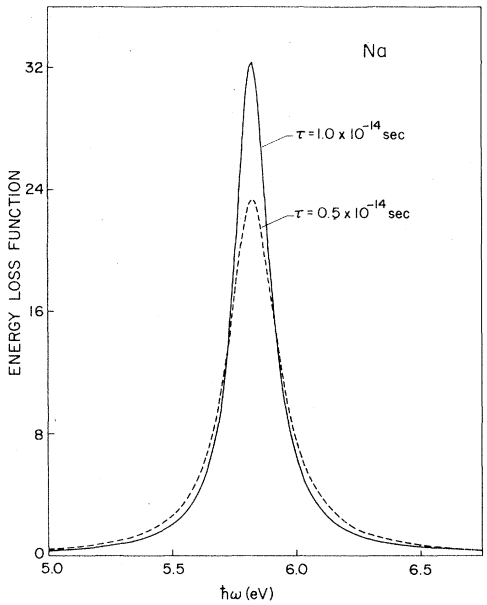

FIG. 10. Plots of the energy-loss function for Na for different scattering times. Here $\epsilon_0 = 1.057$, $m_{op} = 1.02\, m_e$, and $m^* = 1.0\, m_e$.

$1.025 m_e$, a static dielectric function of $\epsilon_0 = 1.04$, and the first three sets of reciprocal-lattice vectors. As in Sec. III, the calculation uses 2-PW's and the procedure of AS. The same formulas were also applied to Na using the parameters listed in Table III.

As noted, the subsequent agreement with experimental observations is within the accuracy of our calculation. The experimental results for the $q = 0$ plasma frequency and FWHM are 14.95 and 0.5 eV, respectively.[35,36] For aluminum we can therefore conclude that a single phenomenological relaxation time is sufficient to describe the electronic response from the visible to at least the near ultraviolet limit of the $q = 0$ plasmon, $\hbar\omega_p(0)$.

The corresponding experimental quantities for Na are not so firmly established.[32,36] Thus values of $\hbar\omega_p(0) = 5.70$ eV and $\hbar\omega_p(0) = 6.05$ eV with corresponding measurements of the FWHM as 0.25 and 0.4 eV, respectively, have been reported. By comparison, our computations yield $\hbar\omega_p(0) = 5.86$ eV and FWHM = 0.24 eV for a scattering time of 0.5×10^{-14} sec. Improved instrumental resolution may eventually reduce the observed FWHM in Na. Generally, very accurate experimental values for Na are hard to obtain and this may account for our slightly less than sterling agreement.

We should note here that the exact position of the plasmon energy in our calculation is dependent on several parameters, namely, m^*, m_{op}, ϵ_0, and τ. The least important of these is the relaxation-time dependence: $\hbar/\tau$ is typically on the order of a

hundredth of an eV. However, for Al the difference between $\epsilon_0 = 1.0$ and 1.04 results in a shift of 0.3 eV. Similarly, the use of a larger value for m_{op} which might reflect additional IB contributions (see Sec. III above) can also alter $\omega_p(0)$. Thus $m_{op} = 1.64 m_e$ gives $\omega_p(0) = 15.05$ eV. Finally, a shift in m^* from 1.025 to 1.05 reduces $\omega_p(0)$ by 0.1 eV.

In summary, a direct inclusion of a relaxation time in a number-conserving manner has allowed us to justify the older theory of Ehrenreich and Phillipp with only slight modifications. An interesting result of the present method is the appearance of an IB contribution to the dc conductivity. In addition, the number conserving procedure has allowed us to examine the effect of scattering on both the local field and on energy-loss line shapes in simple metals. We have found good agreement between theory and experiment in our calculations of the plasma frequency and FWHM's. Finally, for those systems which are well described by a weak pseudopotential, we find that the plasmon line shape is dominated mainly by IB transitions and the choice of a scattering time, the local field having relatively slight effect.

ACKNOWLEDGMENTS

We would like to thank P. B. Allen and B. Chakraborty for very helpful conversations. This work was supported by the National Science Foundation (Grant No. DMR 77-18329) and through the Cornell Materials Science Center (Grant No. DMR-76-81083), Technical Report No. 4079.

APPENDIX

We provide here explicit formulas for $\epsilon(\omega)$ of Sec. III and the integrals in Eq. (28). The general method for setting up the problem of direct IB transitions in a 2-PW model for the case where parallel bands (PB) exist has been sketched in AS. We follow the same procedure here in dividing Fourier reciprocal space into regions which can undergo a direct IB transition and those portions of the Fermi sea which are forbidden on IB transition through a reciprocal-lattice vector $\vec{K}$ by the Pauli principle.

Writing $\sigma_{PB}(\omega)$ for the PB conductivity and $\sigma_{IB}(\omega)$ for "normal" IB conductivity (i.e., of the Butcher-Wilson form) we find

$$\sigma_{PB}(\omega) = \sum_K{}' \frac{\sigma_a(a_0K)n_K}{i\pi a_K}\{-2\tan^{-1}(x^2-1)^{1/2}\,|_1^{z_0} + [f(a_K,x)+f(-a_K,x)]\,|_1^{z_0}\}$$
$$\times\,\theta(\mathcal{E}_F - |V_K| - \tfrac{1}{4}\mathcal{E}_K^0), \qquad a_K = \hbar(\omega + i/\tau)/2|V_K|$$

$$\sigma_{IB}(\omega) = \sum_K{}' \frac{\sigma_a(a_0K)}{i\pi a_K} n_K \frac{V_K}{\mathcal{E}_K}\Big(z_1(z_0^2-1)^{1/2} - z_0(z_1^2-1)^{1/2} + (z_1-z_0)[\tan^{-1}(z_0^2-1)^{1/2} - \tan^{-1}(z_1^2-1)^{1/2}]$$
$$-\frac{1}{2a_K}[(z_0-a_K)(z_1+a_K)f(a_K,x)\,|_{z_0}^{z_1} - (z_1-a_K)(z_0+a_K)f(-a_K,x)\,|_{z_0}^{z_1}]\Big),$$

and

$$\epsilon(\omega) = 1 - \frac{\omega_{op}^2}{\omega(\omega+i/\tau)} + \frac{i4\pi}{\omega}[\sigma_{PB}(\omega)+\sigma_{IB}(\omega)].$$

Here $\mathcal{E}_F$ is the Fermi energy, $\mathcal{E}_K = \hbar^2K^2/2m$, $\sigma_a = e^2/24\pi\hbar a_0$, the prime on the sums indicates $K=0$ to be excluded, and the limits $|_{z_0}^{z_1}$ or $|_1^{z_0}$ indicate that the complex functions

$$f(a,x) = -\frac{1}{(a^2-1)^{1/2}}\ln\left(\frac{-(1+ax)+[(a^2-1)(x^2-1)]^{1/2}}{a+x}\right),$$
$$f(-a,x) = -\frac{1}{(a^2-1)^{1/2}}\ln\left(\frac{-(1-ax)+[(a^2-1)(x^2-1)]^{1/2}}{x-a}\right)$$

are to be considered indefinite integrals of x to be evaluated between the K-dependent limits. These limits are given by

$$z_0 = \left|\frac{2(\mathcal{E}_K\mathcal{E}_F + V_K^2)^{1/2} - \mathcal{E}_K}{2V_K}\right|,$$

and

$$z_1 = \frac{\mathcal{E}_K + 2(\mathcal{E}_K\mathcal{E}_F + V_K^2)^{1/2}}{|2V_K|}.$$

Furthermore, the factor n_K denotes the number of equivalent lattice vectors of length K. Finally we rec-

ognize the Heaviside function

$$\theta(x)=\begin{cases}1 & \text{if } x\geq 0\\ 0 & \text{if } x<0\end{cases}$$

as indicating when the PB structure contributes.

In the same notation the integrals of Eq. (28) are

$$\mathfrak{B}_{0\vec{K}}=-2[f(a_{\vec{K}},x)+f(-a_{\vec{K}},x)]\Big|_1^{z_0}\theta(\epsilon_F-\tfrac{1}{4}\epsilon_{\vec{K}}^0-|V_{\vec{K}}|)+\frac{1}{a_K|V_K|}\,\frac{4\epsilon_F-\epsilon_{\vec{K}}}{4}[f(a_{\vec{K}},x)-f(-a_{\vec{K}},x)]\Big|_{z_0}^{z_1}$$
$$-[f(a_{\vec{K}},x)+f(-a_{\vec{K}},x)]\Big|_{z_0}^{z_1}+\frac{|V_{\vec{K}}|}{\mathcal{E}_{\vec{K}}a_{\vec{K}}}\left(2a_{\vec{K}}\ln\left|\frac{z_1+(z_1^2-1)^{1/2}}{z_0+(z_0^2-1)^{1/2}}\right|-(a_{\vec{K}}^2-1)[f(a_{\vec{K}},x)-f(-a_{\vec{K}},x)]\Big|_{z_0}^{z_1}\right),$$

$$\mathfrak{B}_{\vec{K}\vec{K}}=\frac{|V_{\vec{K}}|}{\mathcal{E}_{\vec{K}}}[2(z_0^2-1)^{1/2}+a_{\vec{K}}^2[f(a_{\vec{K}},x)+f(-a_{\vec{K}},x)]\Big|_1^{z_0}]\theta(\mathcal{E}_F-\tfrac{1}{4}\epsilon_{\vec{K}}^0-|V_{\vec{K}}|)$$
$$+\frac{4\mathcal{E}_F-\mathcal{E}_{\vec{K}}}{4\mathcal{E}_{\vec{K}}}\left(\ln\left|\frac{z_1+(z_1^2-1)^{1/2}}{z_0+(z_1^2-1)^{1/2}}\right|-\frac{a_{\vec{K}}}{2}[f(a_{\vec{K}},x)-f(-a_{\vec{K}},x)]\Big|_{z_0}^{z_1}\right)$$
$$+\frac{|V_{\vec{K}}|}{\mathcal{E}_{\vec{K}}}\left((z_1^2-1)^{1/2}-(z_0^2-1)^{1/2}+\frac{a_{\vec{K}}^2}{2}[f(a_{\vec{K}},x)+f(-a_{\vec{K}},x)]\Big|_{z_0}^{z_1}\right)$$
$$-\frac{V_{\vec{K}}^2}{2\mathcal{E}_{\vec{K}}^2}\left(z_1(z_1^2-1)^{1/2}-z_0(z_0^2-1)^{1/2}+2a^2\ln\left|\frac{z_1+(z_1^2-1)^{1/2}}{z_0+(z_0^2-1)^{1/2}}\right|-a_{\vec{K}}(a_{\vec{K}}^2-1)[f(a_{\vec{K}},x)-f(-a_{\vec{K}},x)]\Big|_{z_0}^{z_1}\right),$$

and

$$b_{\vec{K}\vec{K}}=\frac{2|V_{\vec{K}}|}{\mathcal{E}_{\vec{K}}}(z_0^2-1)^{1/2}\theta(\mathcal{E}_F-\tfrac{1}{4}\mathcal{E}_{\vec{K}}-V_{\vec{K}})+\frac{4\mathcal{E}_F-\mathcal{E}_{\vec{K}}}{4\mathcal{E}_{\vec{K}}}\ln\left|\frac{z_1+(z_1^2-1)^{1/2}}{z_0+(z_0^2-1)^{1/2}}\right|+\frac{|V_{\vec{K}}|}{\mathcal{E}_{\vec{K}}}[(z_1^2-1)^{1/2}-(z_0^2-1)^{1/2}]$$
$$-\frac{V_{\vec{K}}^2}{2\mathcal{E}_{\vec{K}}^2}\left(z_1(z_1^2-1)^{1/2}-z_0(z_0^2-1)^{1/2}-\ln\left|\frac{z_1+(z_1^2-1)^{1/2}}{z_0+(z_0^2-1)^{1/2}}\right|\right).$$

[1]H. Ehrenreich and H. R. Philipp, Phys. Rev. 128, 1622 (1962).
[2]M. P. Greene, H. J. Lee, J. J. Quinn, and S. Rodriguez, Phys. Rev. 177, 1019 (1969).
[3]N. D. Mermin, Phys. Rev. B 1, 2362 (1970).
[4]N. W. Ashcroft and K. Sturm, Phys. Rev. B 3, 1898 (1971).
[5]N. Wiser, Phys. Rev. 129, 62 (1963).
[6]S. L. Adler, Phys. Rev. 126, 413 (1962).
[7]K. Sturm, Phys. Rev. Lett. 40, 1599 (1978).
[8]K. Sturm, Z. Phys. B25, 247 (1976).
[9]K. Sturm, Z. Phys. B28, 1 (1977).
[10]K. Sturm, Z. Phys. B29, 27 (1978).
[11]P. C. Gibbons, Phys. Rev. B 17, 549 (1978).
[12]G. Paasch, Phys. Status Solidi 38, K123 (1970).
[13]N. W. Ashcroft, Phys. Lett. 23, 48 (1966).
[14]H. Ehrenreich and M. H. Cohen, Phys. Rev. 115, 786 (1959).
[15]N. W. Ashcroft and N. D. Mermin, *Solid State Physics* (Holt, Rinehart, and Winston, New York, 1976).
[16]H. Ehrenreich, in *The Optical Properties of Solids*, edited by J. Tauc (Academic, New York, 1966).
[17]G. A. Rooke, J. Phys. C 1, 776 (1968).
[18]B. Segall, Phys. Rev. 124, 1797 (1961).
[19]V. Heine and M. L. Cohen, in *Solid State Physics*, edited by H. Ehrenreich, F. Seitz, and D. Turnbull (Academic, New York, 1970), Vol. 24.
[20]S. J. Nettel, Phys. Rev. 150, 421 (1966).
[21]D. J. Stevenson, Phys. Rev. B 7, 2348 (1973).
[22]B. Chakraborty and P. B. Allen, Phys. Rev. Lett. 42, 736 (1979).
[23]P. B. Allen, Phys. Rev. B 18, 5217 (1978).
[24]B. Chakraborty and P. B. Allen, Phys. Rev. B 18, 5225 (1978).
[25]A. G. Matthewson and H. P. Myers, J. Phys. F 2, 403 (1972).
[26]D. L. Johnson, Phys. Rev. B 9, 4475 (1974).
[27]S. G. Louie, J. R. Chelikowsky, and M. L. Cohen, Phys. Rev. Lett. 34, 155 (1975).
[28]W. Hanke and L. J. Sham, Phys. Rev. Lett. 33, 582 (1974).
[29]K. Sturm, J. Phys. C 12, 53 (1979).
[30]H. Bross, J. Phys. F 8, 2631 (1978).
[31]P. Zacharias, J. Phys. F 5, 645 (1975).
[32]P. C. Gibbons, S. E. Schnatterly, J. J. Ritsko, and J. R. Fields, Phys. Rev. B 13, 2451 (1976).
[33]D. Pines, *Elementary Excitations in Solids* (Benjamin, New York, 1963).
[34]P. M. Platzman and P. A. Wolff, *Waves and Interactions in Solid State Plasmas* (Academic, New York, 1973).
[35]P. Batson, Ph. D. thesis, Cornell University, 1976 (unpublished); P. Batson and J. Silcox, report (unpublished).
[36]T. Kloos, Z. Phys. 265, 225 (1973).